

Evaluation of an experimental method via numerical simulations

H. Schuler

Fraunhofer Institute for High-Speed Dynamics, Freiburg, Germany

ABSTRACT: In a classical compression or tensile test using a Hopkinson bar, the stress-strain relation is obtained via the strain measurement on the bars. From the signals on the input and output bar the deformation and the stress in the specimen are calculated. In the case of spall experiments, the output bar vanishes and well-established methods cannot be applied. For this reason Schuler et al. 2006 developed a method for the measurement of the tensile strength and fracture energy in a spall experiment. The method is specified and analyzed via numerical simulations within this paper.

1 INTRODUCTION

For the simulation of dynamic processes on concrete structures such as explosions, impacts or penetrations, dynamic material properties are inevitable. The dependence of the strength increase in compression and tension has meanwhile been well-established. A couple of investigations under high strain rate tensile loading have been performed by Klepaczco et al. 2001 and Schuler et al. 2006. An overview of the results of different investigations is given in Figure 1. Dynamic investigations to the fracture energy are seldom found in the literature. Wehrheijm 1992 and Schuler et al. 2006 are two exceptions. In Figure 2 the results of their investigations are shown.

To achieve strain rates higher than 10/s, spall experiments are most frequently used. However they have the disadvantage that the force-deformation relation cannot be measured directly. There is a free end on one side of the specimen. For that reason Schuler et al. 2006 developed a method for determining the tensile strength and fracture energy in a spall experiment. In the first part of this paper the method is described briefly. In the second part, numerical simulations are performed to evaluate this method.

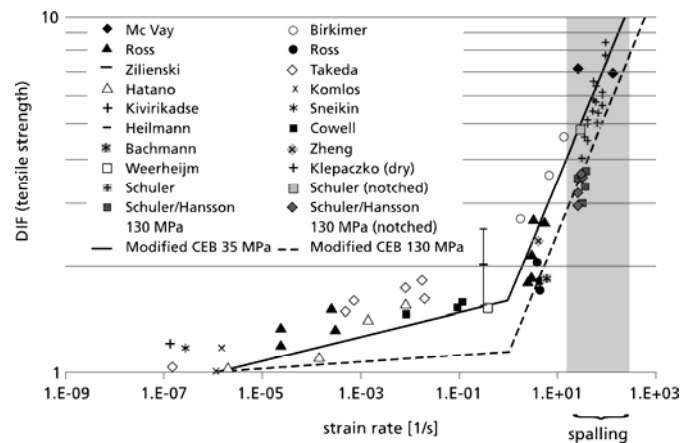


Figure 1: Dynamic tensile strength / static tensile strength (DIF) in dependence of the strain rate.

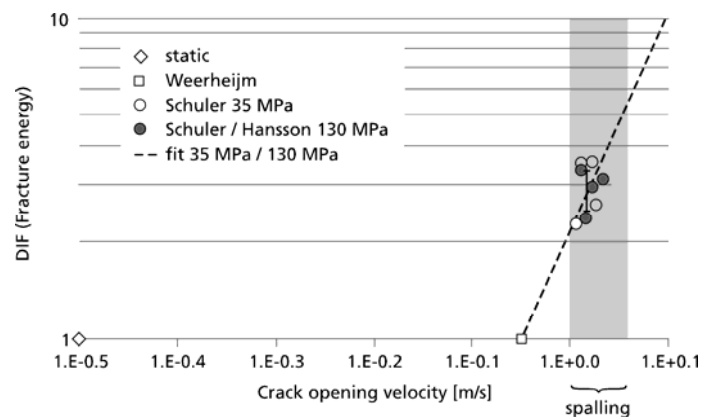


Figure 2: Dynamic fracture energy / static fracture energy (DIF) in dependence of the crack opening velocity.

2 EXPERIMENTAL METHOD

2.1 Tensile strength – plain specimen

In a spall experiment using a Hopkinson bar a projectile is shot on the incident bar. This causes an elastic wave in the incident bar that propagates towards the specimen. The main part of the wave is transmitted into the specimen. At the free end of the specimen the wave reflects and fracture occurs. Figure 3 shows the process of the wave propagation and reflection in a spall experiment.

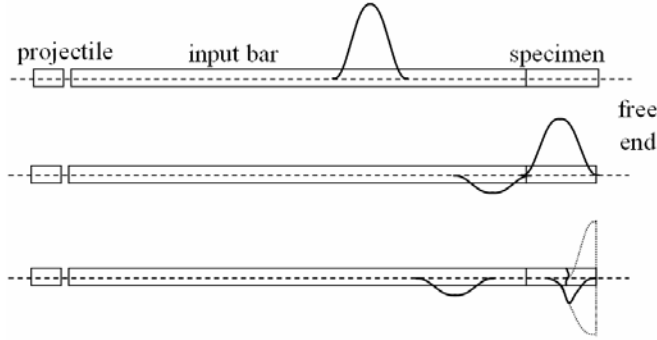


Figure 3: Wave propagation and reflection in a spall experiment using a Hopkinson bar.

From the measured velocity at the rear side of the specimen, the tensile strength is obtained. According to equation 1, the tensile strength f_t is calculated from the pull-back velocity Δu_{pb} (cp. Figure 4), the wave propagation velocity C and the density ρ . This method is known from plate impact experiments and adapted to the Hopkinson bar approach. The longitudinal wave speed for a one dimensional strain state (plate impact) is substituted by the speed for one dimensional stress state (Hopkinson bar). The applicability of this adjustment is investigated in section 3.3 via numerical simulations.

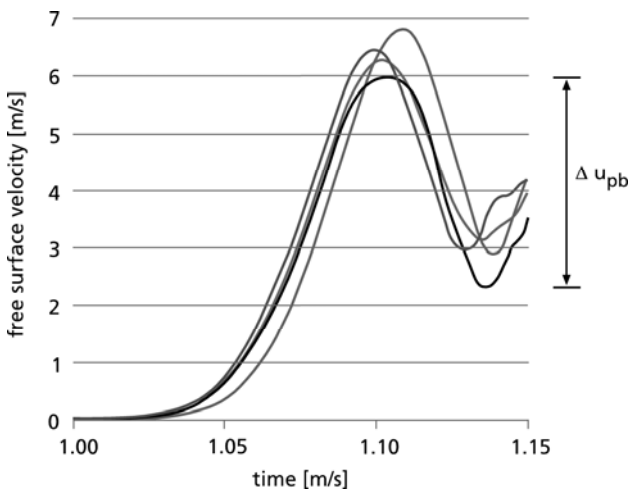


Figure 4: Free surface velocity at the free end of the specimen and pull-back velocity Δu_{pb} for the determination of the tensile strength.

$$f_t = \frac{1}{2} \cdot \rho \cdot C \cdot u_{pb} \quad (1)$$

2.2 Fracture energy – notched specimen

Under the assumption of a 1D stress state and elastic material behavior, the reflection of the wave at the free end of the specimen can be calculated analytically. This is done by setting a mirrored copy at the end of the specimen which is propagating contrary to the original wave (cp. Figure 5). The addition of the imaginary copy with the real wave yields to the shape of the stress $\sigma(x,t)$ and velocity $v(x,t)$ during reflection (cp. Figure 6 and Figure 7). In the case of the stress the sign in the copy has to be changed to minus (-). For the particle velocity the incident and reflected waves have the same sign (+). The corresponding formulas are given in equations 2 and 3.

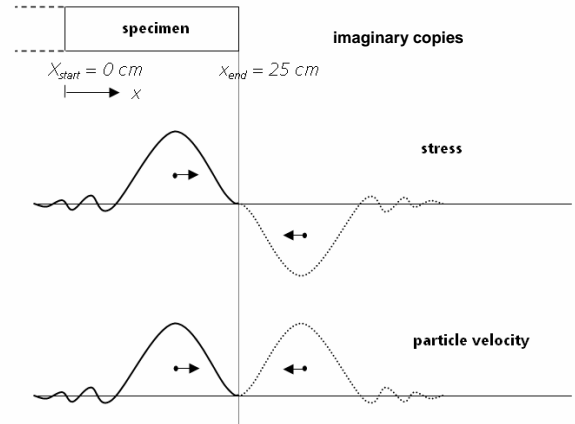


Figure 5: Mirrored copy of the wave (imaginary) for the calculation of the stress and particle velocity during reflection.

$$\sigma(x,t) = \sigma\left(t - \frac{x}{C}\right) - \sigma\left(t + \frac{x - 2x_{end}}{C}\right) \quad (2)$$

$$v(x,t) = \frac{C}{E} \sigma\left(t - \frac{x}{C}\right) + \frac{C}{E} \sigma\left(t + \frac{x - 2x_{end}}{C}\right) \quad (3)$$

During the reflection the compressive stress decreases to zero and the tensile stress increases until tensile strength is reached. The phase of the tensile stress increase is pictured in figure 6. The corresponding particle velocity is given in Figure 7.

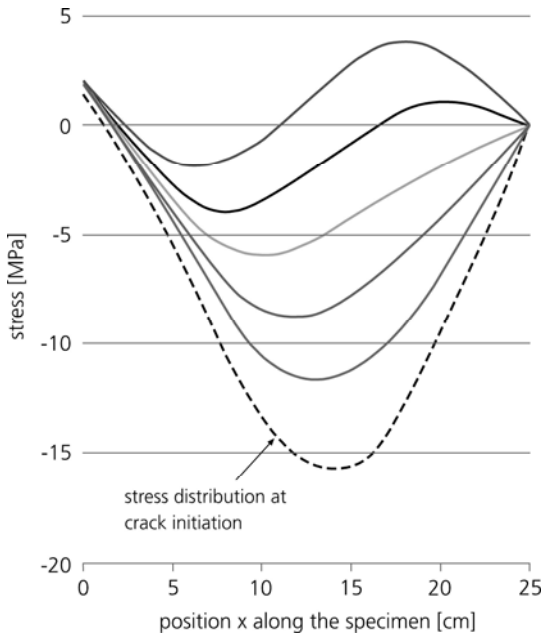


Figure 6: Tensile stress along the axis of the specimen in time steps of two μ s.

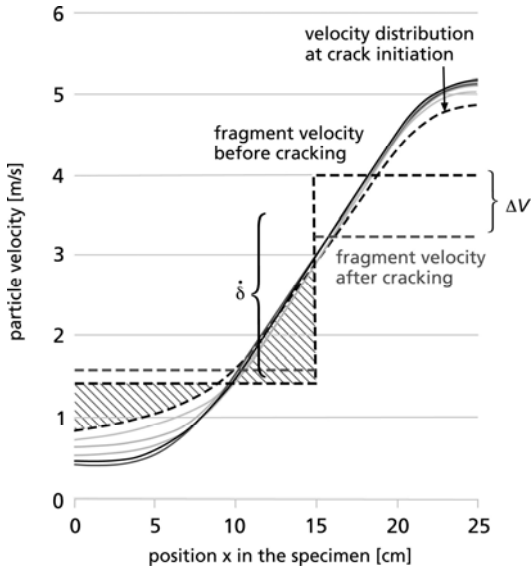


Figure 7: Particle velocity along the axis of the specimen in time steps of two μ s.

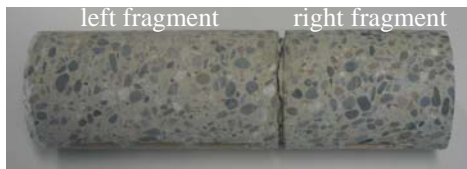


Figure 8: Cracked specimen at the notch and resulting fragments.

At the position where maximum stress occurs (15 cm from the left) a notch is positioned. After the tensile strength is reached, the crack opening process starts at that notch. During this process energy dissipates (fracture energy G_f) which changes the velocity of the two fragments. The left fragment is accelerated and the right one is decelerated. This is shown

in Figure 7 where the mean fragment velocities before and after cracking are shown. The velocities of the fragments “before cracking” are the mean values of analytical calculation in the corresponding section. The velocities “after cracking” are measured via a high-speed camera. From these velocity changes the fracture energy over the whole crack opening process can be calculated according to equation 4. (F = force; δ = crack opening, I = impulse, t = time, m = mass, ΔV and $\dot{\delta}$ according to figure 7)

$$G_f = \int F d\delta = \int \frac{dl}{dt} \dot{\delta} dt \approx m \cdot \Delta V \cdot \dot{\delta} \quad (4)$$

3 NUMERICAL ANALYSIS

3.1 Geometrical model

The Hopkinson bar and the specimen have a diameter of 75 mm. The length of the specimen is 250 mm. The numerical analysis is performed via an axial symmetric calculation with a coarse and a fine discretization. Figure 9 shows the geometrical model of the spall experiment.

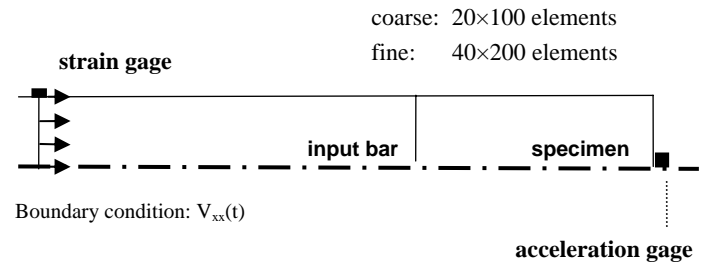


Figure 9: Geometrical model of the spall experiment using a Hopkinson bar.

Instead of simulating the impact of the projectile, a boundary condition is set in the incident bar. The measured signal from the strain gage is applied as a velocity boundary: $v_{xx}(t) = c \cdot \varepsilon_{xx}(t)$. The investigation comprises plain specimens for the measurement of the tensile strength and notched specimens for the measurement of the fracture energy.

3.2 Physical model

The bar consists of aluminum. The material is described with an elastic material description. This is sufficient because the applied stress does not reach the yield strength. The used elastic constants are: Young's modulus: $E = 72.7$ GPa, Poisson Ratio: $\nu = 0.34$. The density is $\rho = 2720$ kg/m³. The same is the case for the behavior of concrete under compression. The wave propagation causes elastic deformation only. The used constants in the model are: $E = 40.0$ GPa and $\nu = 0.2$. The density is $\rho =$

2320 kg/m³. The behavior under tension is described with a fracture energy based model where elastic behavior is assumed until the tensile strength is reached. For the plain specimen the tensile strength is $f_t = 12.5$ MPa. The fracture energy which is important for the notched specimen is set to $G_f = 380$ J/m². This is the mean value of the measured fracture energy (cp. Figure 2 with the static fracture energy of 125 J/m²).

3.3 Tensile strength – plain specimen

The tensile strength is measured from the pull-back velocity, as it is explained in section 2.1. In the simulation this tensile strength is used and the pull-back velocity is compared to the experiment. As Figure 10 shows, the numerical analyzes yield nearly the same pull-back velocity. This show that the proposed method is appropriate and results with a high accuracy can be achieved. The adjustment from planar plate experiment to the Hopkinson bar experiment is valid!

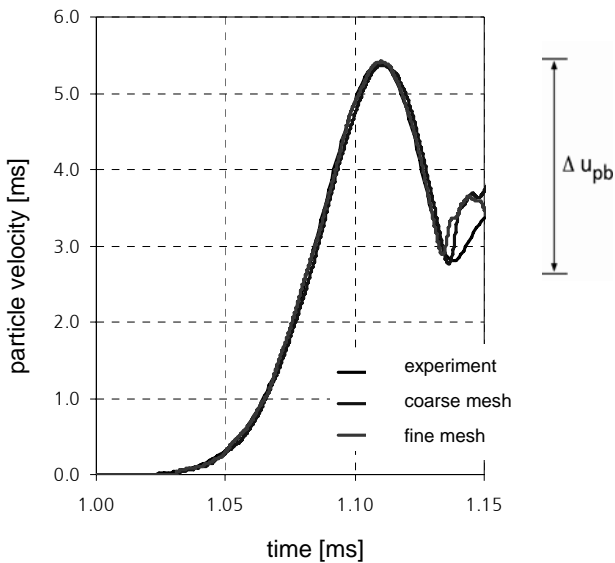


Figure 10: Measured free surface velocity in comparison to the numerical results.

An additional point of interest was the fragmentation of the specimen. Can fragment sizes be calculated? As figure 11 shows, they can. The damage zones from the simulation are at the position where the specimen was broken. The first breach arises at the side near the free end. This is in accordance with the stress development shown in figure 7. The second breach near the incident bar follows later. This is the case for plane specimens when the specimens are glued to the incident bar, which was done for the measurement of the tensile strength.

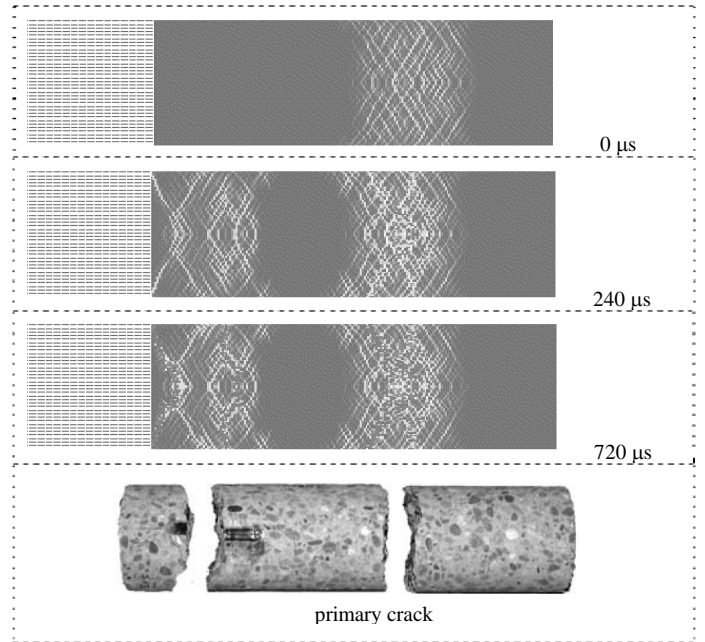


Figure 11: Development of the fracture process in the specimen and fragments in the experiment.

3.4 Fracture energy – notched specimen

For the determination of the fracture energy the specimens were only laid in contact to the incident bar and a notch was cut with a depth of 5 mm. This notch disturbs the propagation of the pressure wave. As Figure 12 shows, a stress concentration emerges at the notch. But the stress does not exceed the elastic limit and no significant damage occurs during the compressive phase. This is a precondition for a spall experiment and is fulfilled. Approximately 40 μs later the tensile stress has reached the strength and the crack opening starts at the notch. The crack propagates towards the center and a release wave follows this propagation (cp. Figure 13). During this time the left fragment is accelerated and the right fragment is decelerated. Figure 14 shows the fragment velocities as a function of time calculated via the numerical simulation. As explained in section 2.2, the fracture energy is determined from the fragment velocities at the time of crack initiation and after the crack is completely opened. Using the time when the crack opening starts at the notch, once obtain with the analytical method a fracture energy of $G_f = 416$ J/m². Using the time when the crack opening start in the center, leads to $G_f = 244$ J/m². The time between initiation at the notch and the center is approximately 6 μs. In the analytical calculation a point of time in between this phase is used which leads to $G_f = 380$ J/m². This shows that using a notch transfers the one dimensional problem to a three dimensional problem which goes along with a few inaccuracies. However, the inaccuracies are in a limited range, which still allow a clear

statement. The investigated dynamic fracture energy is about two to three times the static fracture energy

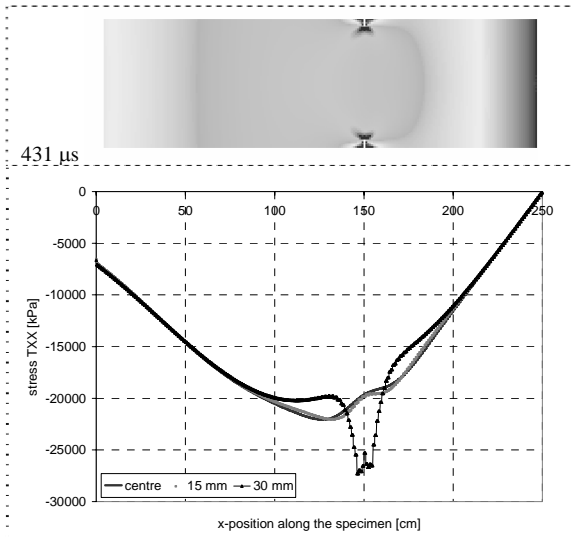


Figure 12: Stress concentration around the notch during the compressive phase; lower figure: stress TXX at a radius of 15 mm and 30 mm.

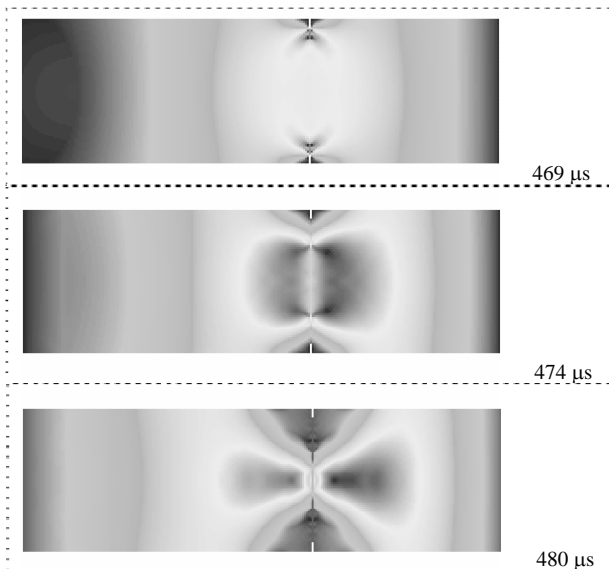


Figure 13: Stress distribution in the specimen during crack opening (propagation of the crack from the notch to the center).

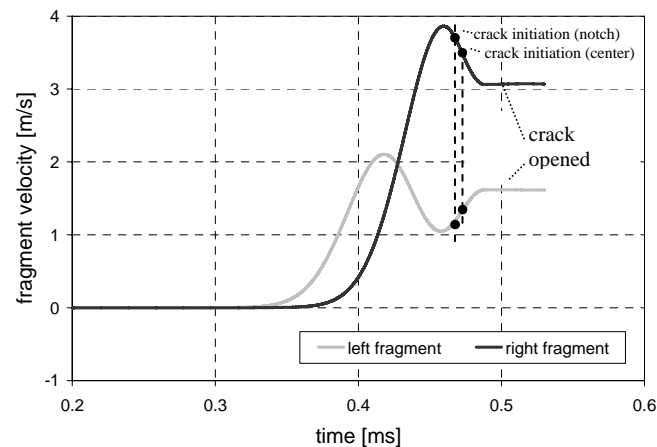


Figure 14: Fragment velocity as a function of time.

4 CONCLUSION

For the measurement of the tensile strength the method used for planar impact experiments is adapted to a Hopkinson Bar spall experiment. The strength is calculated from the pull-back velocity. The numerical analyzes show that with this method the tensile strength can be calculated very precisely. Using the measured tensile strength in the numerical model leads to nearly the same pull-back velocity as in the experiment.

The measurement of the fracture energy is difficult and there exist a few inaccuracies caused by the notch. During the compressive phase a stress concentration arises around the notch. But the stress has an extend which does not cause any damage to the specimen. This is a requirement for spall experiments and is fulfilled. During the tensile phase the assumption of an instantaneous crack initiation over the whole cross section is not correct. The crack propagates from the notch to the center. Depending on which initiation time is used, different fracture energies are calculated. Using the initiation time at the notch, leads to a dynamic increase factor (DIF) of $G_{f,dyn} / G_{f,stat} = 3.33$, using the initiation time in the center $G_{f,dyn} / G_{f,stat} = 1.95$. The factor in the experiment was 3.0. It is difficult to calculate the fracture energy in a spall experiment. However the imprecision of the method is in a range which allows a clear statement: The dynamic fracture energy at high strain rates is two to three times the static fracture energy.

REFERENCES

- Klepaczko, J.R. & Brara, A. 2001. An experimental method for dynamic tensile testing of concrete by spalling, *International Journal of Impact Engineering* 25: 387-409.
- Malvar, L.J. & Ross, C.A. 1998. Strain rate effects for concrete in tension, *ACI Materials Journal* 95(6): 735-739.
- Schuler, H. & Hanson, H. 2006. Fracture Behaviour of High Performance Concrete (HPC) investigated with a Hopkinson-Bar. *Journal de Physique IV*(134): 1145-1151.
- Schuler, H., Mayrhofer, M. & Thoma, K. 2006. Spall experiments for the measurement of the tensile strength and fracture energy of concrete at high strain rates. *International Journal of Impact Engineering* 32: 1635-1650.
- Sluys, L.J. 1992. Wave propagation, localization and dispersion in softening solids, *Dissertation*: Delft University of Technology.
- Weerheijm, J. 1992. Concrete under Impact Tensile Loading and Lateral Compression. *Dissertation*: Delft University of Technology.